Title of Grant / Cooperative Agreement:	Material Ignition and Suppression in Space Exploration Atmospheres
Type of Report:	Summary of Research
Name of Principal Investigator:	Carlos Fernandez-Pello
Period Covered by Report:	1/1/10 - 5/31/13
Name and Address of recipient's institution:	Regents of the University of California, c/o Sponsored Projects Office, Berkeley, CA 94704
NASA Grant / Cooperative Agreement Number:	NNX10AE01G

Reference 14 CFR § 1260.28 Patent Rights *(abbreviated below)*
The Recipient shall include a list of any Subject Inventions required to be disclosed during the preceding year in the performance report, technical report, or renewal proposal. A complete list (or a negative statement) for the entire award period shall be included in the summary of research.

Subject inventions include any new process, machine, manufacture, or composition of matter, including software, and improvements to, or new applications of, existing processes, machines, manufactures, and compositions of matter, including software.

Have any Subject Inventions / New Technology Items resulted from work performed under this Grant / Cooperative Agreement?	No ◉	Yes ○
If yes a complete listing should be provided here: Details can be provided in the body of the Summary of Research report.		

Reference 14 CFR § 1260.27 Equipment and Other Property (abbreviated below)
A Final Inventory Report of Federally Owned Property, including equipment where title was taken by the Government, will be submitted by the Recipient no later than 60 days after the expiration date of the grant. Negative responses for Final Inventory Reports are required.

Is there any Federally Owned Property, either Government Furnished or Grantee Acquired, in the custody of the Recipient?	No ◉	Yes ○
If yes please attach a complete listing including information as set forth at § 1260.134(f)(1).		

Attach the Summary of Research text behind this cover sheet.

Reference 14 CFR § 1260.22 Technical publications and reports (December 2003)
Reports shall be in the English language, informal in nature, and ordinarily not exceed three pages (not counting bibliographies, abstracts, and lists of other media).

A Summary of Research (or Educational Activity Report in the case of Education Grants) is due within 90 days after the expiration date of the grant, regardless of whether or not support is continued under another grant. This report shall be a comprehensive summary of significant accomplishments during the duration of the grant.

NASA GRANT NNX10AE01G

Material Ignition and Suppression Test (MIST) in Space Exploration Atmospheres
Summary of Research

Principal Investigator: Professor Carlos Fernandez-Pello
Department of Mechanical Engineering
University of California
Berkeley, CA 94720-1740

NASA Technical Officer: Dr. David Urban and Dr. Justin Niehaus

Period of Performance: January 1st, 2010– May 31st, 2013

Abstract

The Material Ignition and Suppression Test (MIST) project has had the objective of evaluating the ease of ignition and the fire suppression of materials used in spacecraft under environmental condition expected in a spacecraft. For this purpose, an experimental and theoretical research program is being conducted on the effect of space exploration atmospheres (SEA) on the piloted ignition of representative combustible materials, and on their fire suppression characteristics. The experimental apparatus and test methodology is derived from the Forced Ignition and Flame Spread Test (FIST), a well-developed bench scale test designed to extract material properties relevant to prediction of material flammability. In the FIST test, materials are exposed to an external radiant flux and the ignition delay and critical mass flux at ignition are determined as a function of the type of material and environmental conditions.

In the original MIST design, a small-scale cylindrical flow duct with fuel samples attached to its inside wall was heated by a cylindrical heater located at the central axis of the cylinder. However, as the project evolved it was decided by NASA that it would be better to produce an experimental design that could accommodate other experiments with different experimental concepts. Based on those instructions and input from the requirements of other researchers that may share the hardware in an ISS/CIR experiment, a cylindrical design based on placing the sample at the center of an optically transparent tube with heaters equally spaced along the exterior of the cylinder was developed. Piloted ignition is attained by a hot wire igniter downstream of the fuel sample. Environment variables that can be studied via this experimental apparatus include: external radiant flux, oxidizer oxygen concentration, flow velocity, ambient pressure, and gravity level (if flown in the ISS/CIR). This constitutes the current experimental design, which maintains fairly good consistency with Dr Tien's and Dr Olson's project approaches. A further goal of the project has been to develop a combined solid/gas phase numerical model based on the MIST test methodology to predict the flammability behavior of practical materials in spacecraft.

The Summary of Research report describes the work undertaken in the design of the MIST project as well as initial computational and experimental results. MIST has developed an usable experimental apparatus for evaluation of an optimum configuration of sample, heater and igniter placement to fall within the power supply and heat dissipation requirements of the NASA ISS/CIR. Using this experimental apparatus, preliminary time to ignition and mass loss at ignition data have been collected as a means of establishing a baseline, for eventual use in conjunction with space flight data. In a parallel effort a numerical model of the piloted ignition of a 2-D sample of PMMA has been developed and prediction of ignition delay has been obtained as a function of several ambient variables.

Experimental Task

The current iteration of the experimental apparatus is shown in Figure 1. It is built around a vertically oriented cylindrical sample. Below the sample are a flow chamber, which allows for controlled flows of air with a prescribed oxidizer (balance nitrogen) concentration between 14 and 30 percent at velocities between 10 and 100cm/sec, as well as a flow homogenizer, as per ASTM D2863 − 12. Equispaced around the sample are three infrared halogen lamps capable of irradiating the sample with upwards of 40 kW/m^2 of incident flux. Above the sample, and crossing the boundary layer of the flow is a hot-wire igniter which acts as the source of piloted ignition for the samples. The samples are suspended from the bottom of a milligram accuracy load cell to allow for measurement of the bulk mass loss of the samples as they pyrolyze under the influence of the external radiant flux or while burning.

The apparatus was built to be similar in most respects to the ASTM D2863 - 12[1] standard, and thus the inlet to the test section is filled with borosilicate beads which act to homogenize the flow and produce a uniform flow into the test section. The test section itself is a 254 mm piece of quartz tubing with an outer diameter of 75 mm and an inner diameter of 70 mm. The samples are centered in the test section radially as well as along the lit length of the heaters. The quartz infrared halogen lamp heaters have a lit length of 127 mm and a total length of 220 mm that are enclosed in parabolic reflectors. The three heaters are radially equispaced around the test section at 120 degree intervals, thus irradiating the fuel sample with an approximately uniform heat flux of upwards of 40 kW/m^2. Ignition is induced with an electrically heated Kanthal wire coil that acts as a pilot and is located 25 mm downstream from the trailing edge of the fuel sample. The coil is placed so that it covers the fuel vapor concentration boundary layer thus eliminating the pilot location, in the axial direction, as a parameter of the problem.

Surface temperature of the samples is measured with 0.127 mm wire thickness type K thermocouples placed halfway along the length of the test specimen. Although care is taken to ensure that the thermocouple bead is embedded flush with the sample surface, the measured temperatures presented throughout should only be viewed as an approximation of the actual surface temperature due to movement of the thermocouple resulting from surface density

[1] ASTM D 2863 – 12: “Standard Test Method for Measuring the Minimum Oxygen Concentration to Support Candle-Like Combustion of Plastics (Oxygen Index)”

changes and the growth of pyrolyzate bubbles. The load cell from which the samples are suspended has 0.1 mg resolution. It is positioned above the flow duct, and the specimens are hung, via an auto-centering cup and cone apparatus in the test section to record continuous mass loss data during experiments. Black cast Poly(methyl-methacrylate) (PMMA)type-G samples, approximately 154 mm in length and 12.7 mm in diameter were used for these experiments.

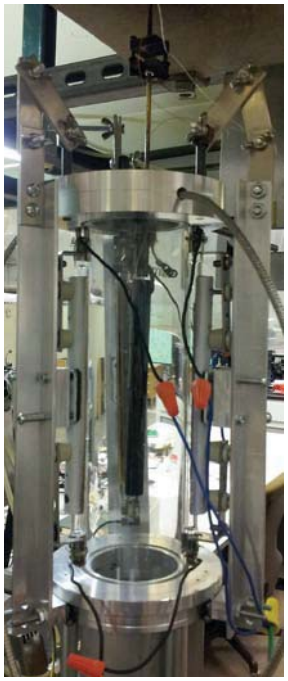

Figure 1: A photograph of the current experimental apparatus

A potential issue of the current MIST experimental design is the dependence of the radiant flux distribution over the sample surface on the number of radiant heaters located around the cylindrical fuel sample. It was determined that differences in surface temperature between samples irradiated by three or four heaters equispaced around the sample was small, which justified the use of three heaters in the experimental design. Simulated surface temperature at an arbitrary point on a samples surface as a function of time for 3 heaters and 4 heaters can be seen in Figure 4. The theoretical results confirm the experimental measurements. Thus it was concluded to finalize the design of the experiment using three radiant heaters as shown in Figure 2. Figures 2 and 3 show the angular variation in heat flux at the surface of a cylindrical sample as a function of power for three and four heaters spaced at 120 and 90° respectively.

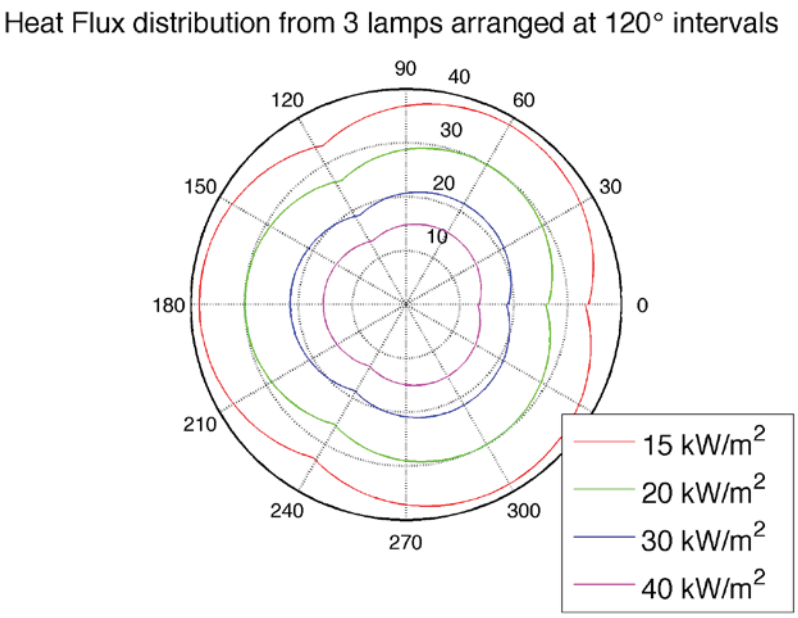

Figure 2: The angular variation in heat flux [kW/m^2] reaching a circular surface given three heaters and 120° heater placement for four different incident power levels

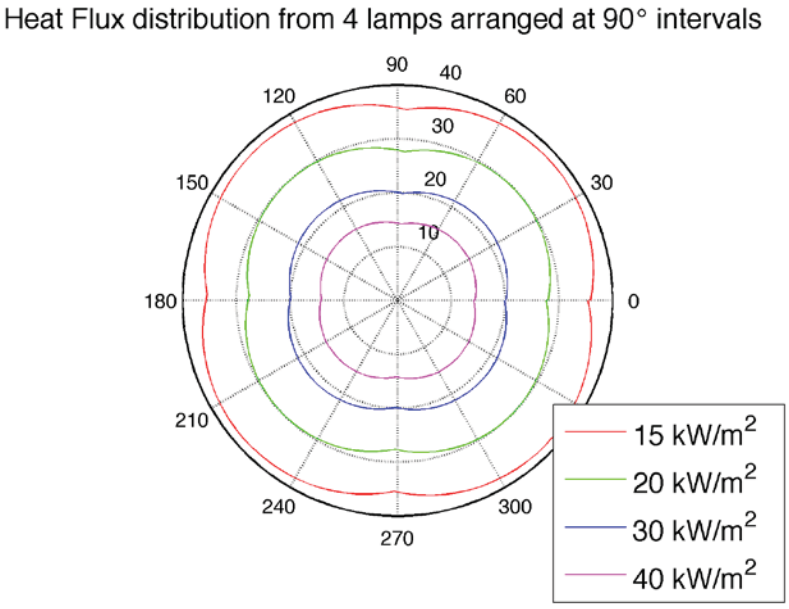

Figure 3: The angular variation in heat flux [kW/m^2] reaching a circular surface given four heaters and 90° heater placement for four different incident power levels

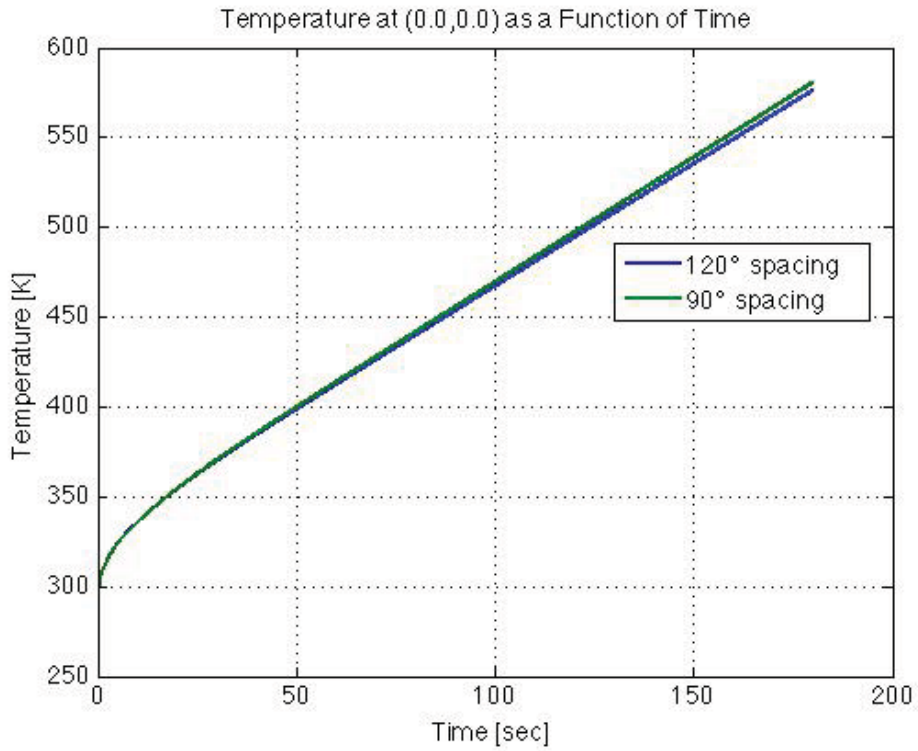

Figure 4: A comparison of simulated surface temperature at an arbitrary point on a sample's surface as a function of time for 3 heaters and 4 heaters given the highest level of power output and no convective cooling.

The construction of the above-described experimental apparatus was finalized and experiments on ignition delay and mass loss at ignition were initiated. Two types of ignition experiments have been conducted with the MIST apparatus. The first set is to determine whether polymer samples, specifically cast PMMA samples, can be re-used so that several ignition tests can be conducted with the same sample. During the tests consideration is given to whether thermal degradation of the samples affects their properties in a significant manner between ignitions, and whether ignition delay in particular is affected. Thus far this investigation has been conducted with piloted ignition of samples similar to those mentioned previously. An example of the experimental results is shown in Figure 5. It is seen that the mass loss before ignition as well as the time to ignition are statistically different between ignition of virgin samples and re-ignition of the same samples after cooling.

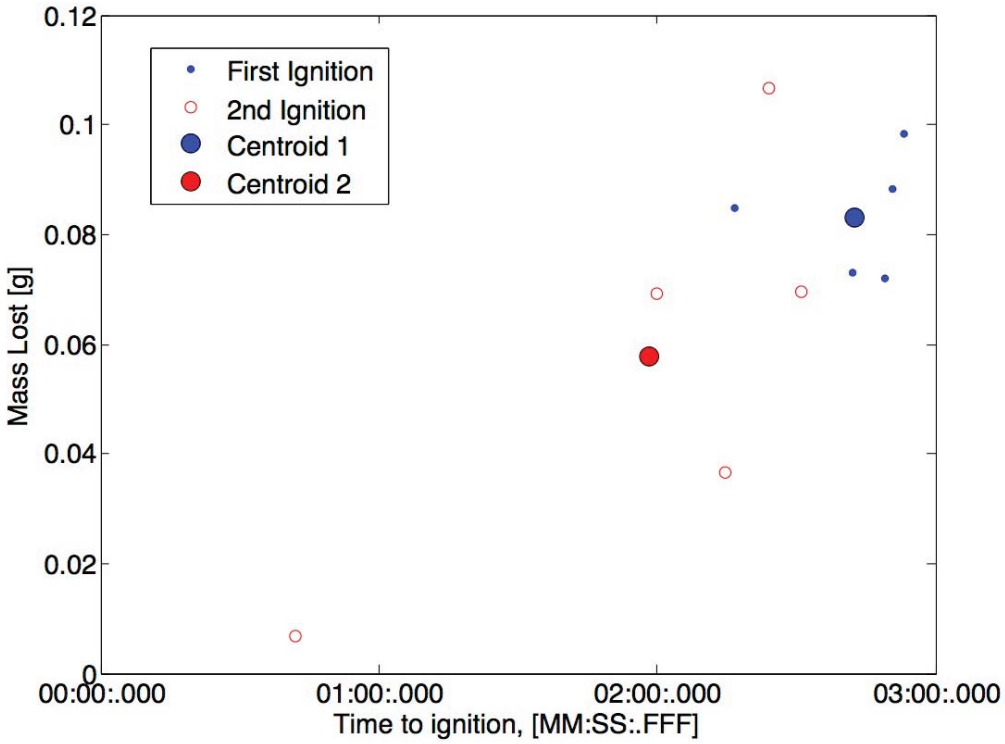

Figure 5: A representative set of re-ignition tests for cast PMMA samples with between 9-11 kW/m^2 incident radiant flux from 3 heaters at 120° spacing with no external flow and ambient atmospheric conditions.

The second set of experiments is aimed at providing ignition delay and mass loss at ignition as a function of the environmental variables. An example unprocessed surface temperature and mass loss data with time is given in Figure 6. The figure presents two sets of data for samples irradiated with ~30 kW/m^2 of incident heat flux under ambient atmospheric conditions. Data such as this can be used to obtain ignition delay and critical mass flux at ignition as a function of the problem parameters. As can be seen in Figure 7, the data seems to indicate an exponential decay in time to ignition with rising heat flux as well as a minimum time to ignition for the given geometrical constraints of the experiment. This was expected given the previous work with the FIST apparatus. Additionally, Figure 8 indicates that across a broad range of incident heat fluxes, at ambient atmospheric conditions, that there is an apparently constant mass loss at ignition.

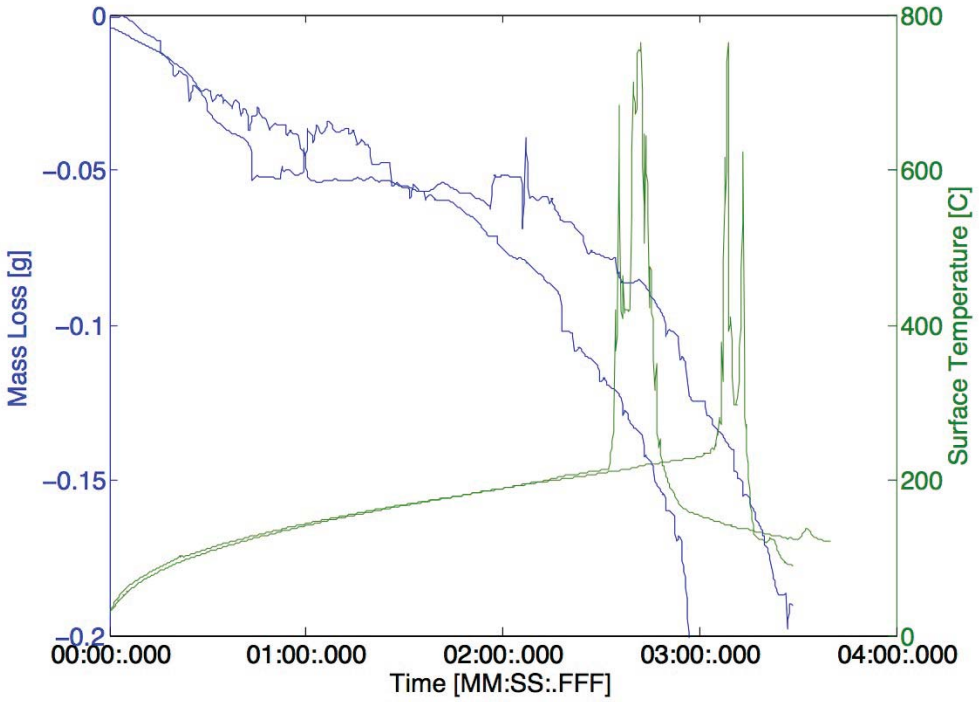

Figure 6: A representative set of ignition tests for cast PMMA samples with between ~30 kW/m^2 incident radiant flux from 3 heaters at 120° spacing with no external flow and ambient atmospheric conditions.

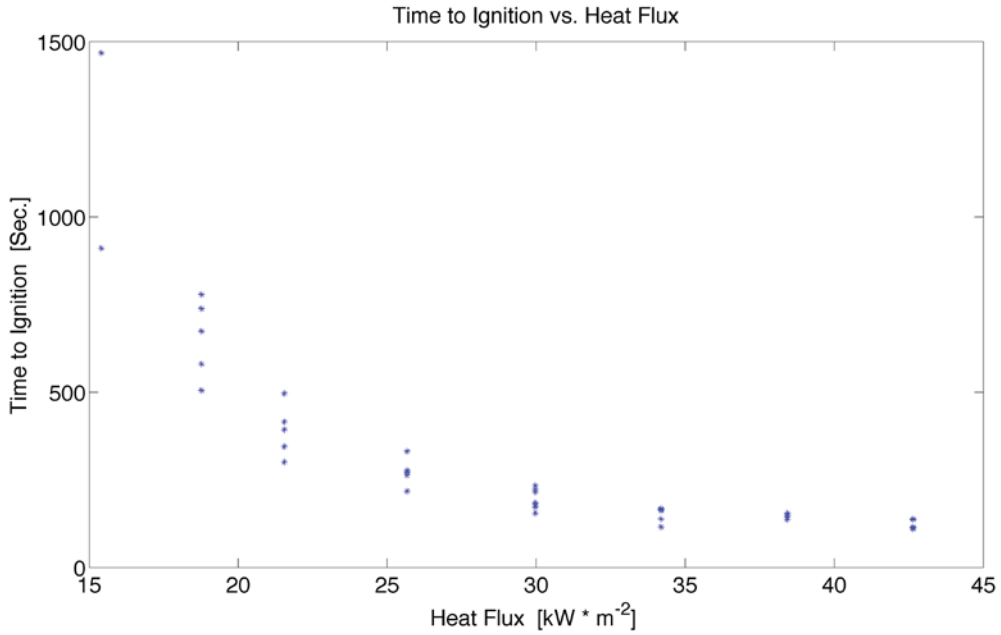

Figure 7: Time to ignition versus incident heat flux for the cast PMMA samples. Each point represents one sample (or test). This data exhibits the expected exponential decay in time to ignition versus incident heat flux as well as indications as to the critical heat flux for ignition and minimum time to ignition.

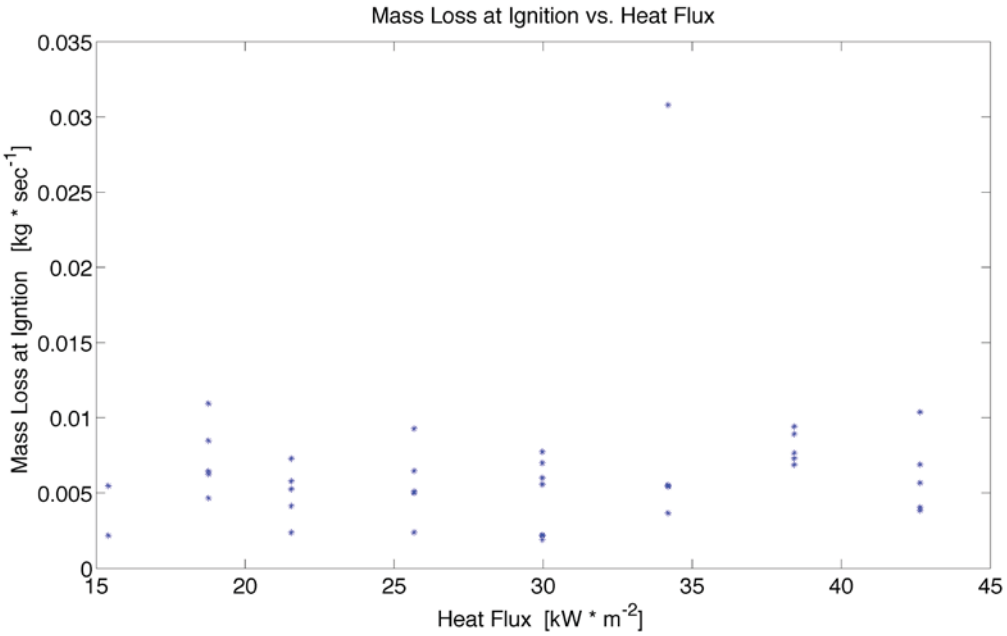

Figure 8: Mass loss at ignition (dm/dt) versus incident heat flux for the cast PMMA samples. As above, each point represents one sample (or test). This data indicates that over a range of heat fluxes that there does not seem to be an appreciable difference in the mass loss at ignition.

Modeling Task

Modeling is being carried out in conjunction with the above experimental work to simulate the MIST experiments. One version of the current model currently in use was developed to simulate a 2-D solid fuel slab using the Fire Dynamics Simulator (FDS) [2] version 6R3 in its Direct Numerical Simulation (DNS) mode. A second considers the geometry of the current experiment using a long axisymmetric fuel rod in a duct similar to that in the current iteration of the experiment. The model simultaneously considers the processes in the solid and in the gas phases. The solid phase decomposition is modeled with a single step global Arrhenius reaction rate. Oxidative pyrolysis is not considered and the in-depth formed pyrolyzate is assumed to flow unrestricted through the solid combustible. The gas phase kinetics are modeled with a single-step second order Arrhenius reaction rate. Although the current model may simulate well the cylindrical experiments, it may be necessary to confirm this and implement any necessary modification.

The ignition process simulation results provide a sequential view of the different events leading to the piloted ignition of PMMA. First looking at some graphical results from the simulated flat slab, Figures 9-11 show snapshots of the numerical results for the heat release rate, gas phase temperature and fuel mass fraction at four representative instants during a simulation for a horizontally placed PMMA sample. The ambient pressure is 100 kPa, the oxygen concentration is 21%, the air flow velocity is 0.4 m/s and the external radiant heat flux is 16 kW/m^2. The complete computational domain is not shown for clarity of presentation. Figure 9shows the heat release rate (HRR) per unit volume, which is proportional to the reaction rate.

The HRR plots show how a gas phase reaction appears first at the pilot location (Fig.9.a), 545 seconds after the external heat flux is activated. At this point the gas phase temperature near the sample surface is relatively low compared to the PMMA pyrolysis temperature (Fig.10.a), and the fuel mass fraction is limited to a thin layer next to the fuel surface (Fig.11.a). The fuel air mixture near the pilot is just above the flammability limit for PMMA. With time the rate of fuel pyrolysis grows (Fig.11.b) and so does the reaction rate region around the pilot (Fig.9.b). At 774.1 seconds the reaction rate 'jumps' upstream onto the solid surface (Fig.9.c) in the form of a premixed flame propagating through a premixed mixture, consuming most of the fuel except in a very narrow layer (quenching layer) near the solid surface. During this propagation process a kind of triple flame is generated. Finally at 788.6 seconds the premixed flame propagates across the whole solid surface and a diffusion flame established over the solid surface (Fig.10.d). The gas phase temperature (Fig.9.d) and the fuel mass fraction (Fig.11.d) are typical of a diffusion flame. Note that buoyancy plays an important role once the flame is established over the PMMA surface because the forced flow velocity is low (0.4 m/s).

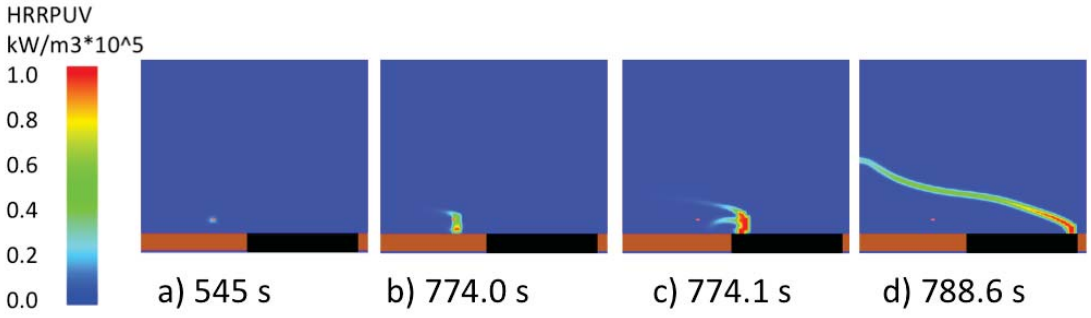

Figure 9: Heat release rate results.

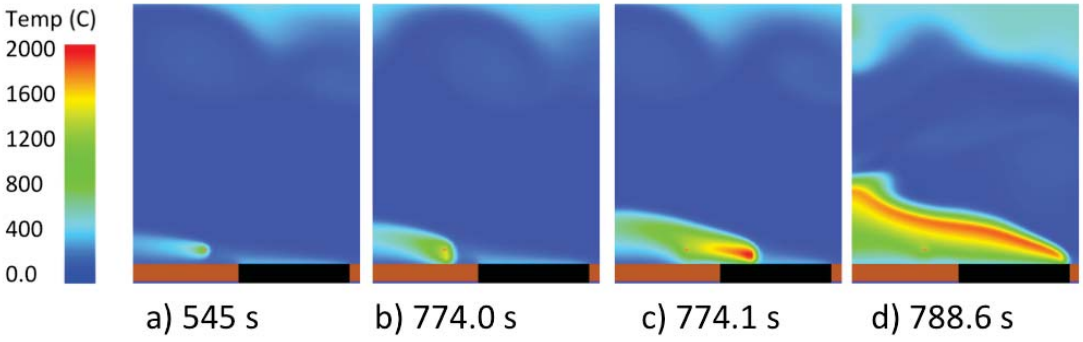

Figure 10. Gas phase temperature results

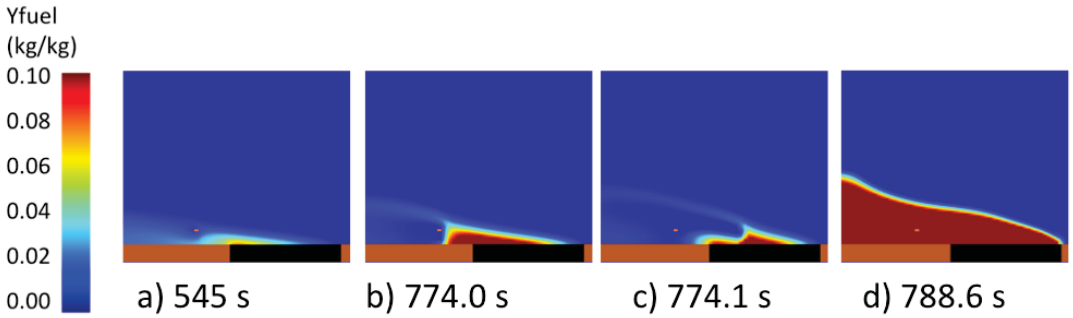

Figure 11. Fuel mass fraction results

Simulations for normal and zero gravity conditions are compared in Figs. 12-13. Figure 12 shows the gas phase temperature at sequential times around the ignition event for 1-g (top) and 0-g (bottom) conditions. The ambient pressure is 100 kPa, the oxygen concentration is 21%, the air flow velocity is 0.4 m/s and the external radiant heat flux is 16 kW/m^2. From Figs. 12a to 12c it is seen that buoyancy plays an important role through the Rayleigh-Taylor instability at normal gravity, particularlyonce the flame is established over the PMMA surface. However, the Rayleigh-Taylor instability disappears for zero gravity conditions (Fig. 12 d, e and f) and the flame shows a distinct round, more uniform shape. Furthermore, ignition occurs significantly earlier at 0-g than at 1-g conditions (596 s compared to 774 s).

Figure 13 shows the heat release rate per unit volume for 1-g (top) and 0-g (bottom) conditions. The HRR snapshots show how the gas phase reaction at the pilot (Fig. 13.a for 1-g, Fig.13.d for 0-g) eventually "jumps" upstream onto the solid surface (Fig.11.b for 1-g, Fig.11.e for 0-g) in the form of a premixed flame propagating through a premixed mixture, consuming most of the fuel except in a very narrow layer (quenching layer) near the solid surface. During this propagation process a type of triple flame is generated (Fig.13.b for 1-g, Fig.13.e for 0-g). At a certain point the premixed flame propagates across the whole solid surface and a diffusion flame is established over the solid surface (Fig.13.c for 1-g, Fig.13.f for 0-g). A distinct feature was observed in the microgravity flame: the reaction was quenched multiple times, jumping from the pilot location onto the surface and back, until it anchored on the solid surface and propagated uniformly towards the leading edge.

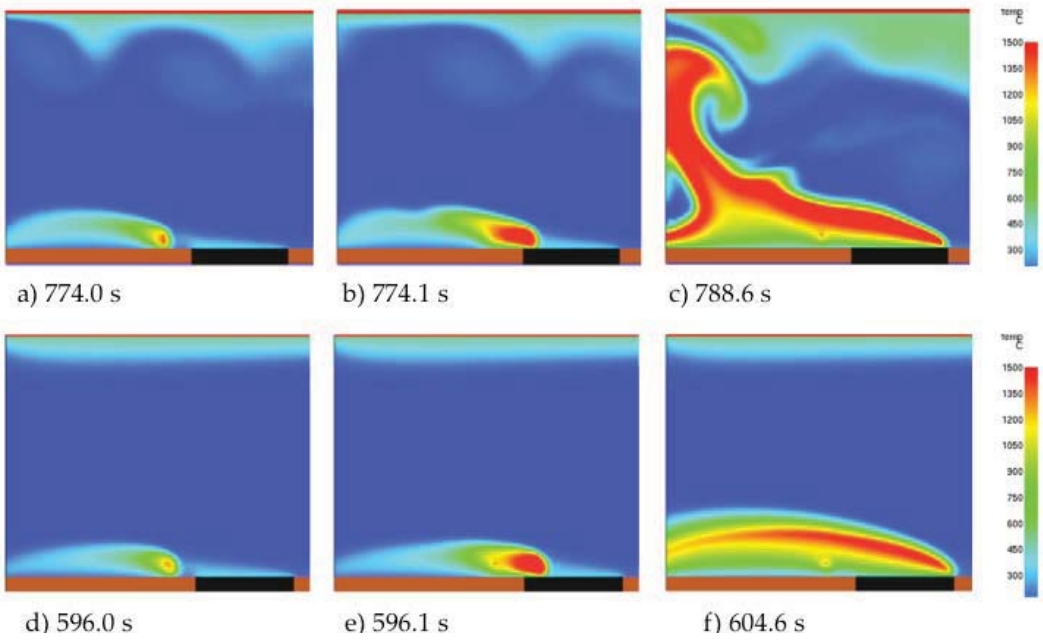

Figure 12. Comparison of gas phase temperature around ignition. Ambient pressure is 100 kPa, air flow velocity 0.4 m/s and q"=16 kW/m2. Top row (a-c) corresponds to 1-g, bottom row (d-f) to 0-g.

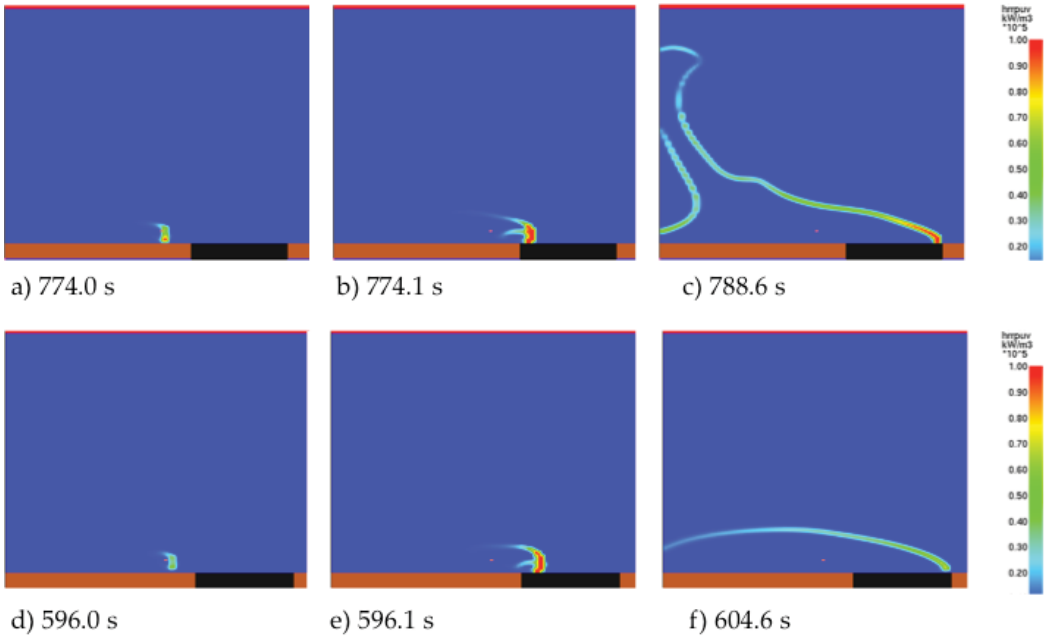

Figure 13. Comparison of heat release rate (HRR) around ignition. Ambient pressure is 100 kPa, air flow velocity 0.4 m/s and q"=16 kW/m2. Top row (a-c) corresponds to 1-g, bottom row (d-f) to 0-g.

Finally, looking at the model of the cylindrical rod samples, as presented in Figures 14 and 15, one can begin to determine the effects that differing heat fluxes have on the cylindrical samples. In Figure 14, the burning rate as a function of time is shown for the same heat flux

range examined experimentally. In comparing this data to the experimental results shown in Figure 8, it can be seen that there is good agreement in the data in the intermediate range of heat fluxes investigated, while the current model seems to over-predict the burning rate at high heat fluxes, and under-predict it for low heat fluxes.

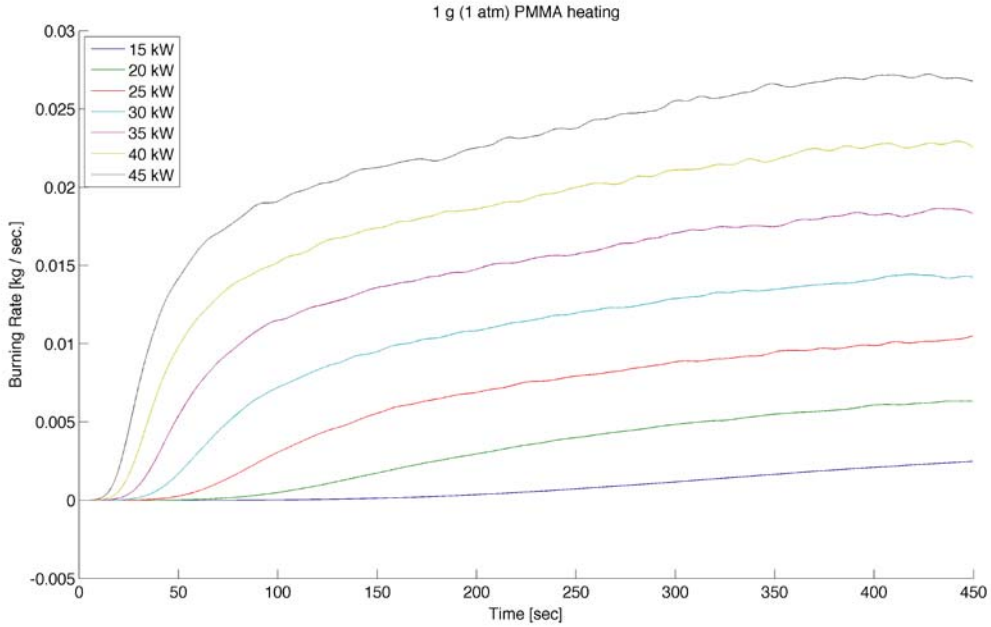

Figure 14. Comparison of calculated burning rates [kg/sec.] as a function of incident heat flux. Ambient pressure is 1 atm, air flow velocity 0.02 m/s.

Similarly, in Figure 15, one can use the computed heat release rate of from the model to determine ignition delay time. These can also be compared to the experimental time to ignition data presented in Figure 7. The current model seems to under predict ignition delay time, and in many cases by a significant amount. This is potentially due to how the incident heat flux boundary condition was imposed as a uniform flux and in it's current incarnation does not account for edge effects due to the finite length of the heater. Another possible concern may be the asymmetry implied by the model, which may not be accounting for the thinner boundary layer of the rod, thus over predicting the convective losses, leading to the sample to heat faster. Generally though, both the flat slab and cylindrical rod models are moving towards becoming useful predictive tools for the study of ignition and flame spread phenomena.

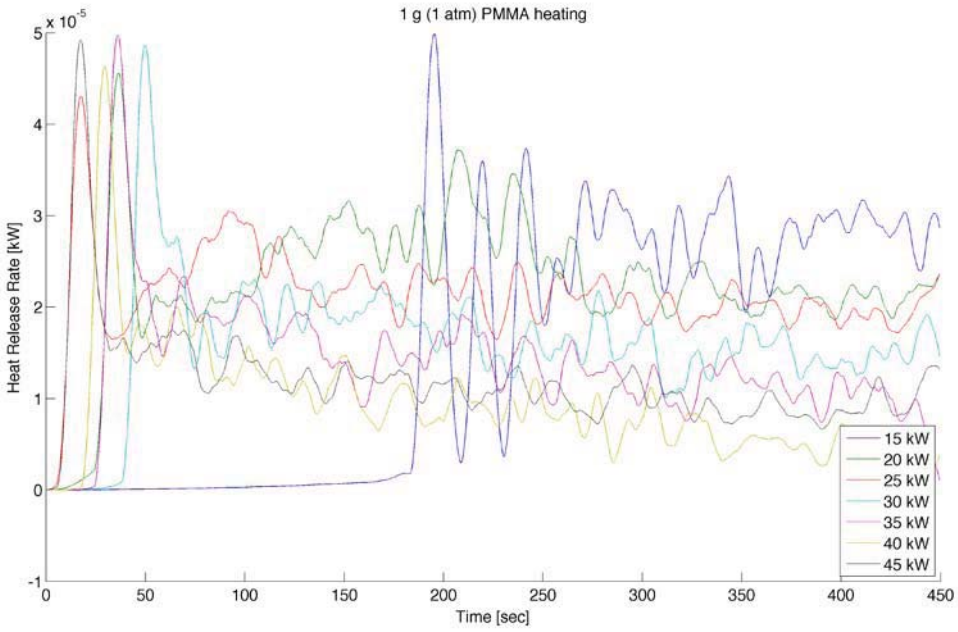

Figure 15. Comparison of calculated heat release rates [kW] as a function of incident heat flux. Ambient pressure is 1 atm, air flow velocity 0.02 m/s.

Publications during this grant period

S. Fereres, C. Lautenberger, C. Fernandez-Pello, D. Urban, and G. Ruff, "Understanding Pressure effects on Piloted Ignition Through Numerical Modeling " *Combustion and Flame*, **159**, 12, 3544-3553 (2012).

S. Fereres, C. Fernandez-Pello, D. Urban and G. Ruff, "Identifying the Roles of Microgravity and Reduced Pressure on the Ease of Ignition of Solid Combustibles" 42nd International Conference on Environmental Systems (ICES), AIAA, San Diego, CA, July 16-18 (2012).